

# **A NEW ELEMENT FOR ANALYSIS OF INTERLAMINAR STRESSES IN LAMINATED COMPOSITES**

K. He, S. V. Hoa & R. Ganesan  
*Concordia Center for Composites,  
Department of Mechanical Engineering,  
Concordia University  
Montreal, Quebec, Canada.*

**SUMMARY:** Based on the identification of globally continuous variables within an overall laminated composite structure as a basic control variable field in Hellinger-Reissner variational principle, a new element - three-dimensional triangular-prism partial-hybrid-stress finite element - has been developed. The element formed based on this scheme exhibits its prominent advantage over the conventional hybrid counterpart element by allowing only three interlaminar stress components to be independently assumed. As a result, the number of the stress parameters required for constructing the element is reduced to half of that for the conventional hybrid element. This yields a significant reduction of computing efforts to obtain the interlaminar stress components, which are of interest in this study. By invoking the consistency of the stress with strain which is compatible with the assumed displacement field, the stress interpolation function that satisfies equilibrium equations and possesses minimum number of stress parameters has been found and further validated to be in suppression of zero-energy deformation through eigenvalue analysis. An example for analysis of interlaminar stresses in the laminate with a hole is illustrated to demonstrate the efficiency and accuracy of the element.

**KEY WORDS:** Laminated composites, interlaminar stresses, partial hybrid elements

## **INTRODUCTION**

The use of fiber-reinforced laminated composites is increasing steadily in a variety of engineering fields. This is largely due to the high specific strength and high specific stiffness displayed by the materials, as well as their tailoring capacity to meet design requirements through variation of fiber orientation and stacking sequence. However, along these properties come complications that must be effectively overcome. One of these involves the resistance of composite laminates to delamination, an interply phenomenon manifesting into a structural premature failure.

It is well known that interlaminar stresses, which usually exist near the traction free edges and/or material discontinuities, play a fundamental role in the initiation and propagation of

delaminations. The importance of interlaminar stresses on the failure characteristics of composites has been demonstrated in many works on this subject. Both numerical and analytical analyses have been performed to determine the magnitude and distribution of the interlaminar stresses. The numerical solutions typically use finite element methods, among which the hybrid stress element, due to assumptions made in the element formulation, appears to be more robust than others with respect to stress analysis of laminates. In hybrid stress element, displacement and stress fields are independently assumed, and stress profiles can be found without further differentiation of displacement variables, and this leads to an increase in computational efficiency. Another aspect attracting researchers is the satisfaction of interelement continuity conditions introduced by this element, which results in better prediction of stresses than displacement based elements. However, the high efficiency and accuracy accompany two difficulties that need to be handled carefully. One of them is the spurious mechanisms induced by stress parameters assumed, and the other is the huge calculation effort required for an inversion of the flexibility matrix to obtain the element stiffness matrix. Both of them are closely related to the number of independent stress parameters ( $m$ ), the number of nodal displacement ( $n$ ) and the number of rigid-body degrees-of-freedom ( $r$ ). It was indicated in Ref. [2] that an ideal number of the stress terms should be chosen such that  $m$  is greater than or equal to  $n-r$ , but subject to the suppression of all kinematic deformation modes. So properly selecting  $m$  is a key process in the development of a new hybrid element. With the above in mind, a 3-D triangular partial hybrid element is developed in the present work. It is formulated based on the modified Hellinger-Reissner variational principle<sup>[1]</sup>. Within this element, only 3 interlaminar stress components ( $\mathbf{s}_z, \mathbf{t}_{yz}, \mathbf{t}_{xz}$ ) that dominate the delamination failure of a composite laminate are assumed, instead of all 6 stress components as used in the conventional hybrid element. Computational time will thus be significantly reduced. The objective of the present study is to establish a simple partial hybrid element that enables an efficient and accurate analysis of stress distribution at the critical region of the laminates. The content covered in this paper includes an introduction of modified Hellinger-Reissner variational principle based on an identification of interlaminar continuity conditions and its resulting partial hybrid element, establishment of 3D triangular prism element, including the determination of the stress shape functions, and an application of the element to the analysis of interlaminar stresses in composite laminates with a central circular hole.

## **MODIFIED HELLINGER-REISSNER VARIATIONAL PRINCIPLE BASED ON IDENTIFICATION OF INTERLAMINAR CONTINUITY CONDITIONS**

Lamination and anisotropy constitute the distinct behavior of the laminated composite structures. They lead to the conjunction conditions at interfaces between adjacent layers in laminated composite structures. In order to satisfy conjunction conditions, the identification of globally continuous variables and locally continuous variables is required. In the laminated composites, all components of displacement, strain, and stress are continuous within each layer

due to the fact that the individual laminae are treated as homogeneous orthotropic material. At the layer interface with perfect bonding, the displacements are also continuous due to the compatibility condition. As a result, the in-plane strains are continuous across the thickness. Meanwhile, the reaction forces give rise to interlaminar stresses and they are also continuous across the thickness because of the equilibrium condition. It is thus seen that the following continuity conditions hold between the stress and strain fields of adjacent layers at their interface:

$$\begin{Bmatrix} \mathbf{e}_x \\ \mathbf{e}_y \\ \mathbf{g}_{xy} \end{Bmatrix}^{(k)} = \begin{Bmatrix} \mathbf{e}_x \\ \mathbf{e}_y \\ \mathbf{g}_{xy} \end{Bmatrix}^{(k+1)} ; \quad \begin{Bmatrix} \mathbf{t}_{xz} \\ \mathbf{t}_{yz} \\ \mathbf{s}_z \end{Bmatrix}^{(k)} = \begin{Bmatrix} \mathbf{t}_{xz} \\ \mathbf{t}_{yz} \\ \mathbf{s}_z \end{Bmatrix}^{(k+1)} \quad (1)$$

By classifying the variables into globally- and locally- continuous variables, both the stress components and strain components can be partitioned into two groups

$$\dot{\mathbf{o}}_l = \begin{Bmatrix} \mathbf{s}_x \\ \mathbf{s}_y \\ \mathbf{t}_{xy} \end{Bmatrix}, \quad \dot{\mathbf{o}}_g = \begin{Bmatrix} \mathbf{s}_z \\ \mathbf{t}_{zy} \\ \mathbf{t}_{zx} \end{Bmatrix}; \quad \dot{\mathbf{a}}_g = \begin{Bmatrix} \mathbf{e}_x \\ \mathbf{e}_y \\ \mathbf{g}_{xy} \end{Bmatrix}, \quad \dot{\mathbf{a}}_l = \begin{Bmatrix} \mathbf{e}_z \\ \mathbf{g}_{zy} \\ \mathbf{g}_{zx} \end{Bmatrix} \quad (2)$$

where subscripts  $g$  and  $l$  denote global and local variables, respectively. Coupling the globally and locally continuous variables results in the new variable vector  $\mathbf{q}$  and  $\mathbf{p}$  as follows

$$\mathbf{q} = \begin{Bmatrix} \dot{\mathbf{a}}_g \\ \dot{\mathbf{o}}_g \end{Bmatrix} \quad \text{and} \quad \mathbf{p} = \begin{Bmatrix} \dot{\mathbf{o}}_l \\ -\dot{\mathbf{a}}_l \end{Bmatrix} \quad (3)$$

in which the negative sign is introduced in order to ensure the symmetry of the coupled constitutive relation.

To construct an element stiffness matrix by the Hellinger-Reissner principle, one has to consider the stationary condition of the following functional:

$$\mathbf{P}_{HR} = \int_V \left\{ -\frac{1}{2} \dot{\mathbf{o}}^T [\mathbf{S}] \dot{\mathbf{o}} + \dot{\mathbf{o}}^T (\mathbf{D} \mathbf{u}) - \mathbf{F}_B^T \mathbf{u} \right\} dV - \int_{S_t} \mathbf{T}^T \mathbf{u} dS_t \quad (4)$$

where  $\mathbf{S}$  are the stresses,  $\mathbf{T}$  is the boundary traction in terms of  $\mathbf{S}$ ,  $[\mathbf{S}]$  the elastic compliance matrix,  $\mathbf{u}$  the element displacements,  $\mathbf{F}_B$  the body force,  $V$  the element volume, and  $S_t$  the boundary of the element. The above functional can be written in partitioned forms of stress and strain variables as

$$\mathbf{P}_{HR} = \int_V \left\{ -\frac{1}{2} [\dot{\mathbf{o}}_l^T \ \dot{\mathbf{o}}_g^T] [\mathbf{S}] \begin{Bmatrix} \dot{\mathbf{o}}_l \\ \dot{\mathbf{o}}_g \end{Bmatrix} + [\dot{\mathbf{o}}_l^T \ \dot{\mathbf{o}}_g^T] \begin{Bmatrix} \mathbf{D}_g \mathbf{u} \\ \mathbf{D}_l \mathbf{u} \end{Bmatrix} - \mathbf{F}_B^T \mathbf{u} \right\} dV - \int_{S_t} \mathbf{T}^T \mathbf{u} dS_t \quad (5)$$

where

$$\dot{\mathbf{o}} = \begin{Bmatrix} \dot{\mathbf{o}}_l \\ \dot{\mathbf{o}}_g \end{Bmatrix} \quad \text{and} \quad \mathbf{D} \mathbf{u} = \begin{Bmatrix} \mathbf{D}_g \mathbf{u} \\ \mathbf{D}_l \mathbf{u} \end{Bmatrix} \quad (6)$$

and

$$\mathbf{D}_g = \begin{bmatrix} \partial/\partial x & 0 & 0 \\ 0 & \partial/\partial y & 0 \\ \partial/\partial y & \partial/\partial x & 0 \end{bmatrix} \quad \text{and} \quad \mathbf{D}_l = \begin{bmatrix} 0 & 0 & \partial/\partial z \\ 0 & \partial/\partial z & \partial/\partial y \\ \partial/\partial z & 0 & \partial/\partial x \end{bmatrix} \quad (7)$$

Thus a modified Hellinger-Reissner variational functional can be established with coupled constitutive matrix  $[R]$

$$\begin{aligned} \mathbf{P}_M = \int_V \{ & \frac{1}{2} \hat{\mathbf{d}}_g^T [R_1] \hat{\mathbf{d}}_g + \frac{1}{2} \hat{\boldsymbol{\sigma}}_g^T [R_3] \hat{\boldsymbol{\sigma}}_g + \hat{\boldsymbol{\sigma}}_g^T [R_2]^T \hat{\mathbf{d}}_g \\ & + \hat{\boldsymbol{\sigma}}_g^T \mathbf{D}_l \mathbf{u} - \mathbf{F}_B^T \mathbf{u} \} dV - \int_{S_t} \mathbf{T}^T \mathbf{u} dS_t \end{aligned} \quad (8)$$

Displacement and interlaminar stress fields are present in this functional. With substitutions of the displacement assumption

$$\mathbf{u} = \{u \quad v \quad w\}^T = [N_1 \quad N_2 \quad \Lambda \quad N_n] \{d_1 \quad d_2 \quad \Lambda \quad d_n\}_e^T = [N] \mathbf{d}_e \quad (9)$$

where  $[N]$  is the matrix of shape functions and  $d_i$  is the element nodal displacement and the assumption of a partial stress field within an element

$$\hat{\boldsymbol{\sigma}}_g = \{\mathbf{s}_z \quad \mathbf{t}_{yz} \quad \mathbf{t}_{zx}\}^T = [P_g] \hat{\mathbf{a}}_e = [\hat{\boldsymbol{\sigma}}_{g1}, \hat{\boldsymbol{\sigma}}_{g2}, \Lambda \quad \hat{\boldsymbol{\sigma}}_{gm}] \{\mathbf{b}_1 \quad \mathbf{b}_2 \quad \Lambda \quad \mathbf{b}_m\}_e^T \quad (10)$$

where  $[P_g]$  is an assumed stress matrix,  $\mathbf{s}_{gj}$  are the partial stress modes, and  $\mathbf{b}_j$  are the corresponding stress parameters, Eqn. (8) can be written in the discretized form

$$\begin{aligned} \mathbf{P}_M = \sum_{e=1}^n \{ & \frac{1}{2} \mathbf{d}_e^T \int_V [B_g]^T [R_1^e] [B_g] dV \mathbf{d}_e + \frac{1}{2} \hat{\mathbf{a}}_e^T \int_V [P_g]^T [R_3^e] [P_g] dV \hat{\mathbf{a}}_e \\ & + \hat{\mathbf{a}}_e^T \int_V [P_g]^T ([B] + [R_2^e] [B_g]) dV \mathbf{d}_e - \mathbf{d}_e^T \int_V [N]^T \mathbf{F}^e dV \\ & - \mathbf{d}_e^T \int_S [N]^T \mathbf{T}^e dS \} \end{aligned} \quad (11)$$

The governing equations of the element and the system can be obtained by the stationary conditions of the functional with respect to stress parameters  $\mathbf{b}$  and node displacements  $\mathbf{d}$ .

## THE 3-D 6-NODE TRIANGULAR PRISM PARTIAL HYBRID ELEMENT

### Shape Functions

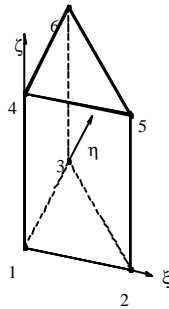


Figure 1: Master triangular-prism finite element

As shown in Figure 1, the proper shape functions are defined as tensor products of two-dimensional shape functions corresponding to the triangular base of the element defined within  $\mathbf{x}, \mathbf{h}$  -plane and one-dimensional shape functions corresponding to the direction  $\mathbf{z}$ . More precisely, if  $\mathbf{y}_1, \mathbf{y}_2$  and  $\mathbf{y}_3$  denote vertex node shape function for a two-dimensional triangular master element and  $\mathbf{j}_1$  and  $\mathbf{j}_2$  are shape function corresponding to vertex nodes of one-dimensional master element, then the three-dimensional shape function can be defined as in the matrix form

$$\mathbf{N} = \begin{bmatrix} \mathbf{y}_1 & \mathbf{y}_2 & \mathbf{y}_3 & 0 & 0 & 0 \\ 0 & 0 & 0 & \mathbf{y}_1 & \mathbf{y}_2 & \mathbf{y}_3 \end{bmatrix}^T \begin{Bmatrix} \mathbf{f}_1 \\ \mathbf{f}_2 \end{Bmatrix} \quad (12)$$

where

$$\mathbf{y}_1 = 1 - \mathbf{x} - \mathbf{h} \quad \mathbf{y}_2 = \mathbf{x}, \quad \mathbf{y}_3 = \mathbf{h}, \quad \mathbf{f}_1 = 1 - \mathbf{z} \quad \text{and} \quad \mathbf{f}_2 = \mathbf{z} \quad (13)$$

### Geometry of Element

For a 3-D 6-node prism isoparametric element, mapping from the global coordinate system (  $x, y, z$  ) to the parametric coordinate system (  $\mathbf{x}, \mathbf{h}, \mathbf{z}$  ) is carried out by

$$x = \sum_{i=1}^6 N_i x_i \quad y = \sum_{i=1}^6 N_i y_i \quad z = \sum_{i=1}^6 N_i z_i \quad (14)$$

where (  $x_i, y_i, z_i$  ) are the global coordinates of the  $i$ -th node (  $i = 1, 2, \dots, 6$  ).

### Displacement Field

As an isoparametric element allows the same geometry and displacement interpolation function, a displacement field, within the element, can be assumed

$$u = \sum_{i=1}^6 N_i u_i \quad v = \sum_{i=1}^6 N_i v_i \quad w = \sum_{i=1}^6 N_i w_i \quad (15)$$

where (  $u_i, v_i, w_i$  ) are the  $i$ -th nodal displacements in the global coordinate system (  $i = 1, 2, \dots, 6$  ), and  $N_i$  are the same shape functions.

### Gauss Integration

The utilized method of numerical integration takes advantage of the so-called symmetrical Gaussian quadrature rule for a triangle<sup>[5]</sup>, applied to longitudinal normalized coordinates  $\mathbf{x}$  and  $\mathbf{h}$  of the master triangle and standard Gauss integration rule applied to the third, transverse normalized coordinate  $\mathbf{z}$  of the one-dimensional master element, which when mixed together form a three-dimensional, symmetrical-standard-product Gaussian integration scheme. Thus, each integrand  $f(\mathbf{x}, \mathbf{h}, \mathbf{z})$  of the stiffness matrix can be integrated according to the rule

$$\begin{aligned} & \int_0^1 \int_0^1 \int_0^{1-h} f(\mathbf{x}, \mathbf{h}, \mathbf{z}) d\mathbf{x} d\mathbf{h} d\mathbf{z} \\ &= \frac{1}{2} \sum_{l=1}^{M_G} \sum_{k=1}^{N_G} w_l w_k f(\mathbf{x}_k, \mathbf{h}_k, \mathbf{z}_l) \end{aligned} \quad (16)$$

where  $N_G$ ,  $w_k$ ,  $\mathbf{x}_k$ ,  $\mathbf{h}_k$  and  $M_G$ ,  $w_l$ ,  $\mathbf{z}_l$  are the number of Gauss points, Gauss point weights and coordinates, for the triangle and the third direction, respectively.

### Interlaminar Stress Interpolation Functions

There are several methods available for obtaining stress modes for hybrid element. With satisfying equilibrium conditions, one  $\mathbf{b}$ -stress term per one  $\mathbf{a}$ -mode scheme<sup>[2]</sup> is applied here to derive the initial interlaminar stress modes. This method can be used to suppress the kinematic deformation and to limit the number of stress modes as minimum as possible. Seven stress modes are available in the stress matrix obtained through this scheme. However, the minimum number of stress modes required for the correct stiffness rank for the element studied is  $m_{\min} = n(3 \times 6) - r(6) - n_d(6) = 6$ , where  $n$ ,  $r$  and  $n_d$  are respectively the number of nodal displacement, the number of rigid-body degrees-of-freedom, and the calculated rank of the semi-stiffness matrix formulated from the globally continuous strains. Therefore, the initial stress matrix needs to be further refined to eliminate one unnecessary mode. Eigenvalue analysis has been applied to obtain the representative modes corresponding to  $m_{\min}$  natural deformation modes<sup>[3]</sup>. The representative stress matrix which assures absence of rank deficiency of the stiffness matrix of the element with the suppression of the zero-energy inducing mode is thus of the form

$$[P_g^*] = \begin{bmatrix} 1 & 0 & 0 & \mathbf{x} & 0 & \mathbf{h} \\ 0 & 1 & 0 & 0 & \mathbf{x} & 0 \\ 0 & 0 & 1 & 0 & 0 & 0 \end{bmatrix} \quad (17)$$

The stress shape functions, thus, provide a constant stress field for each of the three interlaminar stress components, two bending stress fields for the normal stress component  $\mathbf{s}_z$ , and a torsional stress field for the shear stress component  $\mathbf{t}_{yz}$ . The number of stress parameters is two less than that required in the 8-node solid partial hybrid element<sup>[2]</sup>.

Table 1: Results of eigenvalue examination of the element

0.000000	0.000000	0.000000	0.000000	0.000000	0.000000
0.329786	1.161439	1.534557	2.953247	2.988672	3.624301
4.642650	11.215609	12.597004	12.634584	23.687095	72.023983

Parameters used are the same as in the example given below.

## NUMERICAL EXAMPLE

The newly developed element was employed to predict interlaminar stress distribution in a  $[90/0]_s$  composite laminate with a central circular hole subjected to a uniaxial tension in the longitudinal direction.

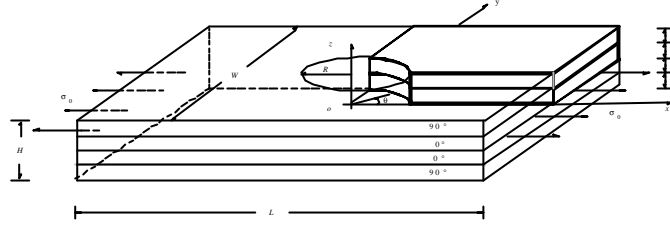


Figure 2: A  $[90/0]_s$  laminate with a circular hole under uniaxial tension

Geometric and material properties for the structure analyzed as shown in Figure 2 are listed in Table 2 and 3. Each ply is treated as a homogeneous elastic and orthotropic as in the case of Raju and Crews<sup>[4]</sup>. Due to the conditions given in the problem, only one-eighth of the laminate needs to be modeled. Two models are considered in this investigation. In model A, each of the plies was represented by one triangular prism element in normal direction, while in model B, two elements were used. A mesh refinement around the hole is required to account for the interlaminar stress singularity expected in this region. The finite element meshes in x-y plane are shown in Figure 3. The minimum length of the element adopted is one half of the ply thickness. The FE model A consists of 292 elements and 642 degrees of freedom, and model B 584 elements and 1128 degrees of freedom. The imposed boundary conditions are  $u(0, y, z) = v(x, 0, z) = w(x, y, 0) = 0$ . Figure 4 and 5 show respectively normalized interlaminar normal stress  $s_z / s_0$  vs  $q$  and normalized interlaminar shear stress  $s_{zq} / s_0$  vs  $q$  for model A and B.

Table 2: Dimensions of the  $[90/0]_s$  Laminate ( mm )

Length	Width	Height	Hole Radius	Ply Thickness
$L = 60$	$W = 30$	$H = .5$	$R = 2.5$	$t = .125$

Table 3: Material properties of the  $0^\circ$  lamina in the  $[90/0]_s$  laminate

Extensional modulus (GPa)	Poisson's ratio	Shear modulus (GPa)
$E_1 = 138$	$\nu_{12} = .21$	$G_{12} = 5.86$
$E_2 = 14.5$	$\nu_{13} = .21$	$G_{13} = 5.86$
$E_3 = 14.5$	$\nu_{23} = .21$	$G_{23} = 5.86$

Subscripts 1, 2 and 3 denote the fiber, transverse and thickness directions, respectively.

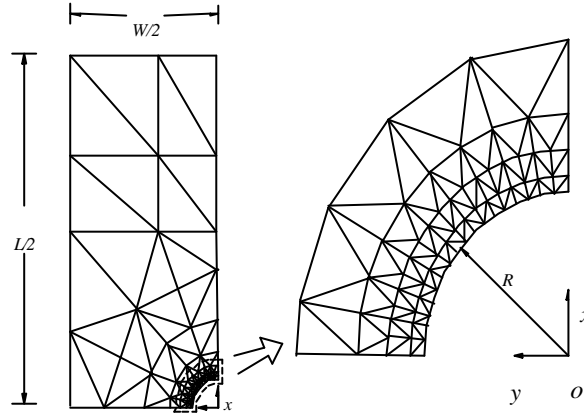


Figure 3: In-plane finite element meshes

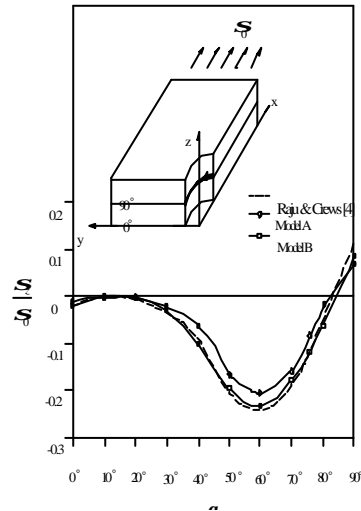




Figure 4: Normalized interlaminar normal stress along  $q$  at the  $90^\circ / 0^\circ$  interface

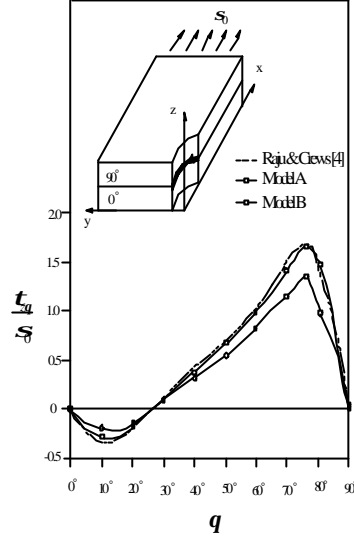


Figure 5: Normalized interlaminar shear stress along  $q$  at the  $90^\circ / 0^\circ$  interface

In figure 4 the distribution of normalized interlaminar normal stress around the hole at the  $90^\circ / 0^\circ$  interface is illustrated for model A and model B, with comparison to the results obtained by Raju & Crews<sup>[4]</sup> based on three-dimensional displacement assumed finite element method. In their model, 20-node isoparametric brick elements consisting of a about 19,000 degrees of freedom that is approximately 15 times as many as in model B were used. A good agreement between the results from the present element and those predicted by Raju & Crews<sup>[4]</sup> can be observed. The same tendency for the stress distribution of  $t_{z\theta}$  can also be observed in figure 5. The shear stress component  $t_{xz}$  is very small compared to the other interlaminar components and can be neglected.

## CONCLUSION

A three-dimensional triangular prism partial hybrid element has been developed based on the identification of interlaminar stress components and in-plane strains as constituting the control variable field in Hellinger-Reissner variational principle. Only three interlaminar stress components are assumed in this scheme. As a result, computational efforts for inverting  $[H]$  and calculating  $[K_h]$  are significantly reduced in comparison with conventional hybrid elements. The initially assumed interlaminar stress field was established first by invoking its consistent with strain which is compatible with the assumed displacement. The optimal interlaminar stress matrix, which possesses the minimum number of stress parameters required for suppression of zero-energy deformation has been found by refining the initial stress field. It has also been validated through demonstrating the absence of rank deficiency for the element stiffness matrix based on the eigenvalue analysis. The number of stress parameters for the present

element considered is only 50 percent of that for a full hybrid stress assumption, and 75 percent of 8-node solid counterpart element. A numerical example for the determination of interlaminar stress distribution in the  $[90/0]_s$  laminate with a central hole was used to illustrate the computational accuracy and efficiency of the new element. It is concluded that accurate solutions to the interlaminar stress distribution in the laminated composites can be predicted by the proposed simple element.

## REFERENCES

1. Hoa, S.V. & Feng, W. *Hybrid Finite Element Method for Stress Analysis of Laminated Composites*, Kluwer Academic Publishers, 1998, USA.
2. Pian, T.H.H. & Chen, D.P. On the suppression of zero energy deformation modes. *Int. J. Num. Meth. Eng.*, **19**, pp. 1741-1752, 1983.
3. Feng, W., Hoa, S.V. & Huang, Q. Classification of stress modes in assumed stress fields of hybrid finite element. *Int. J. Num. Meth. Eng.*, **40**, pp. 4313- 4339, 1997.
4. Raju, I.S. & Crews, J. H., Jr . Three-dimensional analysis of  $[0/90]_s$  laminates with a central circular hole. *Composites Technol. Rev.* 1982, No. 4, (4), pp. 116-24.
5. Reddy, C.T. Improved three point integration schemes for triangular finite elements. *Int. J. Num. Meth. Eng.*, **12**, pp. 1890-1896 (1978).